

# HYDROMECHANICS OF PROPULSION FOR CILIATED MICRO-ORGANISMS

Christopher Brennen

California Institute of Technology

Pasadena, California

## INTRODUCTION

To the present time much of the hydrodynamic analysis of the locomotion of ciliated micro-organisms has concentrated on the localized interaction between the cilia and the fluid medium. In doing so most investigators have found it necessary to simplify the larger scale flow and to consider "infinite sheet models" in which the fluid flow solutions are purely harmonic and the wave properties invariant in the rectilinear coordinate parallel to the sheet. The resulting mean motion is purely unidirectional and thus the hydrodynamic solution greatly simplified. Since these "infinite sheet models" conveniently termed the "envelope" and "sub-layer" models are discussed in detail by Blake and Sleigh (1974a, b) elsewhere in this volume further amplification is unnecessary. It is convenient, however, for our purposes to think of these as fluid/cilia interaction models describing the local interaction between the cilia and the fluid. The relative merits of the two types of model and criteria which describe their respective region of validity are discussed by Brennen (1974) and by Blake and Sleigh (1974b).

In the present paper we will discuss some of the characteristics of the flow around "finite" ciliated micro-organisms, pointing out along the way those effects not experienced in the infinite sheet models but which are important in evaluating, say, the propulsive velocity of a ciliated micro-organism. The only previous solution for a "finite" body to appear in the literature seems to be that of Lighthill (1952), later modified by Blake (1971a) in which traveling surface waves on a sphere (to use the

"envelope" model) are approximated by combining two spherical harmonic functions whose orders differ by one. But this solution is very restrictive in terms of the permitted variation of wave-form and wave amplitude over the body and its extension to non-spheroidal bodies would involve prohibitive algebraic complexity.

Here we take a quite different approach to the rectilinear propulsion of a ciliated organism and make use of some general characteristics of the resulting flow illustrated in Figure 1 and described in more detail by Brennen (1974). The primary simplification arises from the observation that the unsteady components of fluid motion resulting from the interaction between the cilia beating so as to produce a metachronal wave (wave number,  $k = 2\pi/\lambda$ ) and the fluid are attenuated like  $e^{-ky}$  with distance  $y$  from the surface. Such attenuation can also be recognized in the experimental measurements of Cheung and Winet (1974). It follows that, if the metachronal wavelength,  $\lambda$ , is much smaller than the overall dimension of the organism,  $a$ , i. e.  $ka \gg 1$ , then virtually all of the unsteady fluid motions are confined to a thin layer surrounding the organism. This we will term the oscillating-boundary-layer. It follows that outside this layer there is a matching steady flow around the organism created by its steady translation through the fluid at a velocity,  $U$ . This exterior flow is termed the complementary Stokes flow, since the Reynolds number  $Ua/\nu$  ( $\nu =$  kinematic viscosity of the fluid) is generally very much less than unity. A basic philosophy for the solution of the general hydrodynamic problem now becomes apparent. Equations will first be derived which describe the properties of the flow within the oscillatory boundary layer as a function of the ciliary beat and the

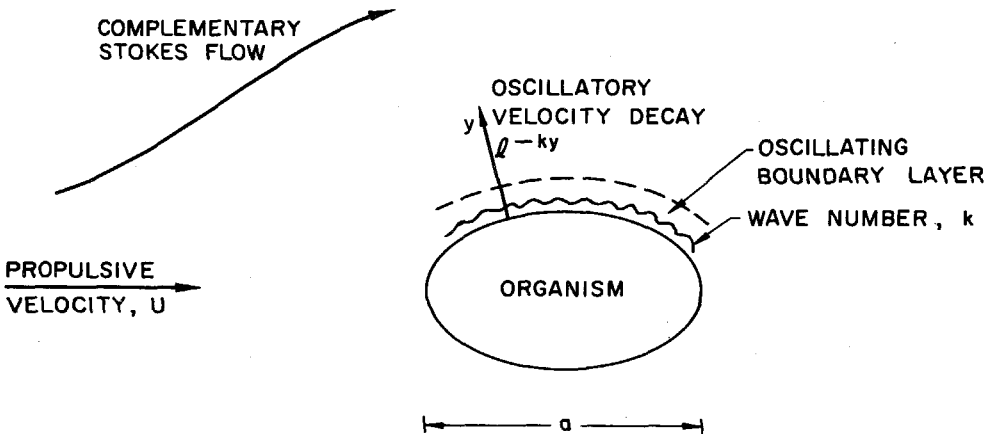


Figure 1. Schematic illustrating the application of the oscillatory boundary layer technique.

metachronal wave parameters. This will then be matched to the complementary Stokes flow in order to determine the latter. If the final objective is to evaluate the propulsive velocity,  $U$ , there is however one final point which must be resolved. Clearly one could add to the complementary Stokes flow any arbitrary Stokes flow which in a frame of reference relative to the organism has zero velocity in the neighborhood of the surface but which arbitrarily changes the velocity at infinity or propulsive velocity,  $U$ . This arbitrariness can only be removed by application of the condition that the total force on the organism be zero, a condition fundamental to self-propelling bodies. In order to implement this condition it is necessary to evaluate the surface stresses on the organism from the oscillatory boundary layer equations (see the section on Equations for the Oscillatory Boundary Layer). The final step in the determination of the propulsive velocity will then be the application of the zero total force condition.

It is worth pointing out that such a philosophy is independent of the particular fluid/cilia interaction model which one chooses to employ. Hence, though we shall confine ourselves here to the development of boundary layer equations for the envelope model, it should be appreciated that boundary layer equations for the sub-layer model could also be developed and a similar procedure adopted.

#### WAVEFORM AND WAVE AMPLITUDE

Since boundary layer equations for the envelope model of fluid/cilia interaction are to be described here it is first necessary to define the motions of that envelope in parametric terms. The motions of a hypothetical material point on the envelope correspond to the motions of a tip of a cilium and, through the conditions of no-slip and impermeability, to the motions of the fluid element at that point. This motion is comprised of displacements both normal (coordinate,  $n$ ) and tangential (coordinate,  $s$ ) to the mean surface. We shall make the assumption that the frequency,  $\omega$ , of ciliary beat and therefore of the displacements is invariant over the mean surface. Thus the metachronal wave can be decomposed into a wave of displacement normal to the surface (the  $n$  wave) of amplitude,  $\Delta n$ , and a wave of displacement tangential to the surface (the  $s$  wave) of amplitude,  $\Delta s$ . Thus at any point,  $s$ , on the surface it is necessary to define three wave quantities, namely a wave amplitude, the ratio of the two amplitudes and the phase between the  $s$  and  $n$  waves. The ratio of amplitudes is defined by the parameter  $K(s)$  where

$$K = [ |\Delta s|^2 - |\Delta n|^2 ] / [ |\Delta s|^2 + |\Delta n|^2 ] \quad (1)$$

so that  $K = +1$  describes a purely tangential displacement (see Tuck (1968)) and  $K = -1$  a purely normal displacement (see first order solution in Taylor (1951)); all other combinations are conveniently bracketed in  $-1 < K < 1$ . We also define a phase angle,  $\theta_p(s)$ , where the  $n$  wave lags the  $s$  wave by  $(\theta_p - \pi/2)$ . Thus the waveform is completely defined by  $K(s)$ ,  $\theta_p(s)$ ; however, it is also convenient from the mathematical point of view to define an alternative waveform parameter,  $\tau(s)$ , which is complex and related to  $K$ ,  $\theta_p$  by

$$K = -\frac{(\tau + \bar{\tau})}{(1 + \tau\bar{\tau})} ; \quad \tan \theta_p = \frac{j(\tau - \bar{\tau})}{(\tau\bar{\tau} - 1)} \quad (2)$$

where the bar denotes complex conjugate and  $j$  is the imaginary index. Figure 2 demonstrates how the locus of an envelope element or ciliary tip varies with  $K$  and  $\theta_p$ . Finally we also define a non-dimensional wave amplitude,  $A(s)$ , such that

$$|\Delta s|^2 = A^2(\tau - 1)(\bar{\tau} - 1)/k^2 ; \quad |\Delta n|^2 = A^2(\tau + 1)(\bar{\tau} + 1)/k^2. \quad (3)$$

It is also convenient to define a length,  $\ell$ , as

$$\ell^2 = |\Delta s|^2 + |\Delta n|^2 = 2A^2(\tau\bar{\tau} + 1)/k^2. \quad (4)$$

Experience with particular cilium beat patterns (Brennen (1974)) indicates that in general  $\ell$  is between 0.5 and 0.8 times the length of the cilium. Hence  $\ell$  will be called the "equivalent cilium length".

### INFINITE SHEET

It is instructive to report here the results of the hydrodynamic solution for the case of an infinite sheet. Brennen (1974) has shown that under the condition that the envelope wave amplitude is small compared with the wavelength the solution of the unsteady Stokes flow equations leads to a propulsive velocity

$$U/c = A^2[\tau\bar{\tau} - \tau - \bar{\tau} - \beta^{-1}] \quad (5)$$

where  $c$  is the metachronal wave velocity and  $\beta = \left\{ \frac{1}{2} [1 + W^2]^{\frac{1}{2}} + 1 \right\}^{\frac{1}{2}}$  where  $W$  is the oscillatory Reynolds number,  $\omega/k^2\nu$ . When the latter is much less than unity,  $\beta \rightarrow 1$  and the solution is identical to that of Blake (1971b). It is worth pointing out that in this case the complementary Stokes flow is simply a uniform stream; moreover from simple momentum principles (as pointed out by Taylor (1951)) the mean or steady component of force on the infinite sheet in the direction of motion must be zero if the fluid motion is

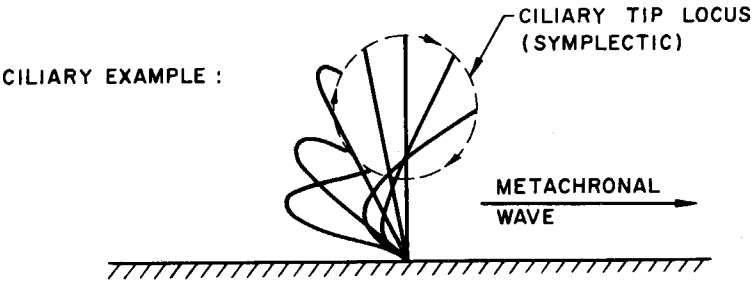
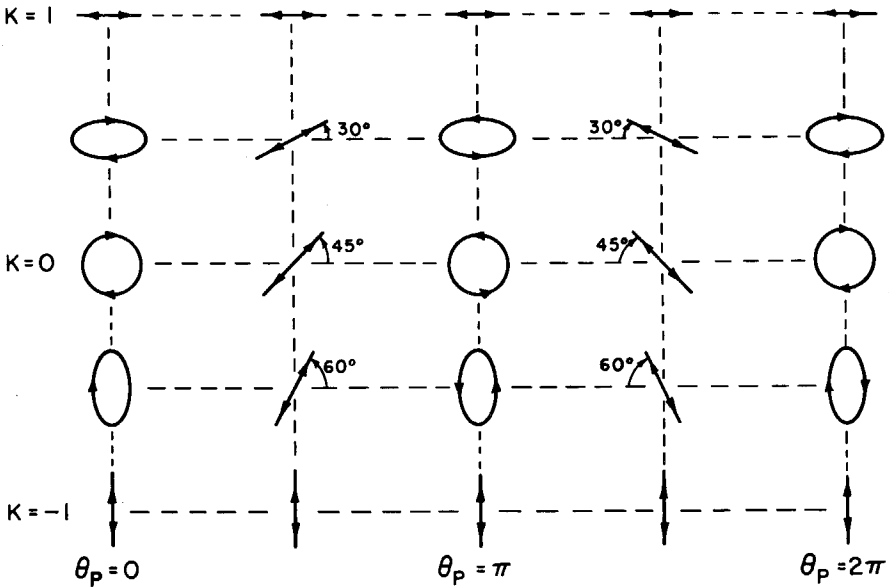


Figure 2. Diagram demonstrating how the elliptic locus of a surface particle varies with changes in the parameters  $K$ ,  $\theta_p$ . Loci are shown for  $K = -1$  to  $+1$  in steps of  $0.5$  and for  $\theta_p = 0$  to  $2\pi$  in steps of  $\pi/2$ . The figure is correlated with the mean surface horizontal, the fluid above it and the surface waves traveling to the right. An example of a cilia tip locus (symplectic) is indicated below.

unsheared far from the sheet. Thus, from the point of view of the discussion in the introduction the infinite sheet is a degenerate example in which the form of the complementary Stokes flow is obvious, a priori, and the zero total force condition is satisfied by implication.

The energy expenditure per unit surface area,  $\dot{E}$ , required to produce the motion is given by

$$\dot{E} = 2\mu kc^2 A^2 [\beta + \tau \bar{\tau}] \quad (6)$$

where  $\mu$  is the dynamic viscosity. Hence we may evaluate the propulsive velocity per unit energy expenditure which when  $W \rightarrow 0$  is simply related to the propulsive velocity divided by  $\ell^2$ :

$$\frac{U}{ck^2 \ell^2} = \omega \mu \frac{U}{\dot{E}} = -\frac{1}{2} \frac{[\tau \bar{\tau} - \tau - \bar{\tau} - 1]}{[\tau \bar{\tau} + 1]} = \frac{1}{2} [(1-K^2)^{\frac{1}{2}} \cos \theta_p - K] \quad (7)$$

and is a function only of waveform given alternatively by  $\tau$  or by  $K$  and  $\theta_p$ . Values are shown in Figure 3 and demonstrate an antiplectic optimum at  $K = 1/\sqrt{2}$ ,  $\theta_p = \pi$  and a symplectic optimum at  $K = -1/\sqrt{2}$ ,  $\theta_p = 0$ . Such results show little dependence on  $W$  being virtually the same at  $W = 1$ ; of course,  $W$  must be significantly less than unity for the basic equations to be valid.

### EQUATIONS FOR THE OSCILLATORY BOUNDARY LAYER

Equations for the oscillatory boundary layer can be developed by generalizing the infinite sheet solution to evaluate the situation in which both the waveform,  $\tau$ , and the wave-amplitude,  $A$ , are slowly varying functions of position,  $s$  on the surface. One then obtains the following boundary conditions, which the

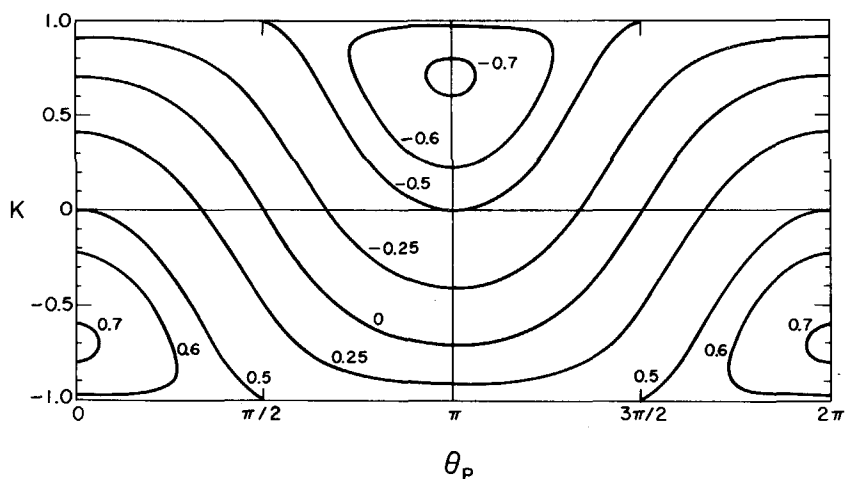


Figure 3. The variation of the propulsive velocity,  $U/ck^2 \ell^2$  or  $\omega \mu U/\dot{E}$ , with waveform type given by  $K$ ,  $\theta_p$  for the infinite flat sheet solution when  $W \rightarrow 0$ . Contours for marked values of  $U/ck^2 \ell^2$  or  $\omega \mu U/\dot{E}$  are shown.

complementary Stokes flow must obey on the mean surface of the organism (Brennen (1974)):

$$q_s = -cA^2 \Sigma_1 ; \tag{8}$$

$$q_n = \frac{\partial}{\partial s} (cA^2 \Sigma_2 / k) \tag{9}$$

where as  $W \rightarrow 0$

$$\Sigma_1 \rightarrow \tau \bar{\tau} - \tau - \bar{\tau} - 1 ; \quad \Sigma_2 \rightarrow 3 - \tau \bar{\tau} / 2 . \tag{10}$$

Expressions for  $W \neq 0$  are also given by Brennen (1974). Here  $q_s$  and  $q_n$  are the components of velocity tangential and normal to the mean surface. Thus, given the waveform,  $\tau(s)$ , and wave amplitude,  $A(s)$  for a particular organism one can construct the steady complementary Stokes flow which satisfies these surface velocity conditions. This, of course, still presents a difficult hydrodynamic problem, though the recent work of Blake and Chwang (1974), Chwang and Wu (1974a, b) and others in the construction of such solutions from distributions of fundamental singularities can be most useful in this regard.

This complementary Stokes flow will, of course, still contain an unknown velocity at infinity or propulsive velocity,  $U$ , which must be obtained from the zero total force condition. For the purposes of evaluation, it is convenient to divided the force on the organism into two components (i) a force due to the complementary Stokes flow,  $F^c$ , which is readily evaluated in the conventional manner and (ii) a force,  $F^p$ , due to the particular solution within the oscillatory boundary layer. It has been demonstrated (Brennen (1974)) that the latter may be obtained by integration of the following tangential ( $\sigma_s$ ) and normal ( $\sigma_n$ ) stresses over the mean surface:

$$\sigma_s = \frac{\partial}{\partial s} (\mu c A^2 \Sigma_3) ; \quad \sigma_n = \frac{\partial}{\partial s} (\mu c A^2 \Sigma_4) \tag{11}$$

where as  $W \rightarrow 0$

$$\Sigma_3 \rightarrow -2j(\tau - \bar{\tau}) \quad ; \quad \Sigma_4 \rightarrow 2(1 - \tau \bar{\tau}) \tag{12}$$

Thus knowing  $\tau(s)$  and  $A(s)$  the force  $F^p$  may be obtained and, from the condition  $F^p + F^c = 0$ , the velocity of propulsion,  $U$  may finally be evaluated. Note that the stresses  $\sigma_s$ ,  $\sigma_n$  and thus the force  $F^p$  are automatically zero in the infinite sheet case since  $A$  and  $\tau$  are then constants.

## CONTRIBUTIONS TO THE PROPULSIVE VELOCITY

It is instructive, before passing to examples of the implementation of the method described here, to review and interpret physically the hydromechanical contributions to the propulsive velocity. All of the contributions to the steady motion occur as quadratic combinations of terms involving the oscillatory motions. The first and primary contribution in the envelope model which has long been realized by Taylor (1951), Blake (1971a, b) and others arises simply from the kinematic surface condition or, in practical mathematical terms, from the quadratic combination of first order oscillatory motions in the second term of a Taylor expansion about the mean position of the surface. When  $W \rightarrow 0$  this is the only remaining effect in the infinite sheet solution (5) and in the oscillatory boundary layer condition (8). When  $W \neq 0$  there is an additional contribution from quadratic combinations in the convective inertial terms for the Navier-Stokes equations but since this is order  $W$  times the kinematic surface condition contribution it is usually small.

An important result of the present method of analyzing a "finite" ciliate is to demonstrate the fact that an additional contribution arises from the surface stresses (11) which contributes (through the zero total force condition) a term to the propulsive velocity which is of the same order as the kinematic surface condition contribution. This additional effect is absent in the "infinite models" since there  $\sigma_s = \sigma_n = 0$ . Thus the application of "infinite model" results to "finite" micro-organism can be significantly in error. Some simple examples will help to illustrate this additional effect and to evaluate the magnitude of the error in infinite model predictions.

## PROPULSION OF AN ELLIPSOIDAL CILIATE

Some simple examples of the application of the oscillating boundary layer theory to the propulsion of a spherical body were given by Brennen (1974). Rather than beginning with some waveform,  $\tau$ , and amplitude,  $A$ , varying over the surface in some specified manner, the examples were simplified algebraically by assuming a complementary Stokes flow of the simplest form namely a spherical harmonic function of the first order. Though this implied certain functional restrictions on the variation of  $\tau$  and  $A$  over the surface, further complexity was deemed unnecessary at the present time since there is little observational information on the variation of ciliary beat pattern with position on a micro-organism. Two particular examples were explored; in the first the waveform,  $\tau$ , remained constant over the surface and the amplitude  $A$  varied in such a way as to allow matching through



the relations (8), (9). The more realistic second example assumed a uniform "equivalent cilium length",  $\ell$  (equation (4)) while the waveform,  $\tau$ , varied. It was most significant that in the neighborhood of optimum propulsion, whether antiplectic or symplectic, the contribution of the "finite body terms" mentioned in the last section enhanced propulsion over that which would be predicted on the basis of an "infinite model".

In the present paper we present a further example by applying the method to an ellipsoidal shaped ciliate propelling itself in the direction of its major axis. The mean shape is assumed to be a prolate ellipsoid given by

$$\frac{x^2}{a^2} + \frac{r^2}{b^2} = 1, \quad a \geq b, \quad e = \left(1 - \frac{b^2}{a^2}\right)^{\frac{1}{2}} \tag{13}$$

A tangent to the surface at any point subtends an angle,  $\varphi$ , with the x axis given by  $\tan \varphi = -b^2 x/a^2 r$ . As in the sphere examples we now choose the simplest complementary Stokes flow consistent with our requirements. This is given in its most appropriate form by Chwang and Wu (1974b), and is constructed using a uniform distribution of stokeslets of strength,  $\alpha$ , oriented in the negative x direction and a parabolic distribution of doublets whose strength is represented by the parameter,  $\beta$ , along the interval of the x-axis between the foci,  $x = \pm ea$ . The resulting flow has tangential and normal velocities on the surface given by

$$q_s = \cos \varphi \left[ U + \frac{2\alpha}{e} - 2(\alpha + \beta)L_e - \frac{2(1-e^2)}{e} \left( \alpha - \frac{2e^2\beta}{(1-e^2)} \right) \right] \tag{14}$$

$$q_n = -\sin \varphi \left[ U + \frac{2\alpha}{e} - 2(\alpha + \beta)L_e - \frac{2}{e} \left( \alpha - \frac{2e^2\beta}{(1-e^2)} \right) \right] \tag{15}$$

where  $L_e = \ln\{(1+e)/(1-e)\}$ ,  $U$  is the propulsive velocity and we must find values for the unknowns  $U$ ,  $\alpha$  and  $\beta$ . Restricting solutions to the case in which the "equivalent cilia length",  $\ell$  is constant over the body it follows from equation (4) and the application of the boundary conditions that

$$\frac{(\tau \bar{\tau} - \tau - \bar{\tau} - 1)}{(1 + \tau \bar{\tau})} = -E \cos \varphi. \tag{16}$$

$$\frac{(3 - \tau \bar{\tau} / 2)}{(1 + \tau \bar{\tau})} = \frac{F b \cos \varphi}{[b^2 \cos^2 \varphi + a^2 \sin^2 \varphi]^{\frac{1}{2}}} + D \tag{17}$$

where  $D$  is an arbitrary integration constant and the constants

$$E = + \frac{2}{k^2 \ell^2 c} [ U - 2(\alpha + \beta)L_e + 2e(\alpha + 2\beta) ] \tag{18}$$

$$F = - \frac{2kb}{k^2 \ell^2 c} [ U - 2(\alpha + \beta)L_e + \frac{4e\beta}{(1-e^2)} ] \tag{19}$$

The relations (16) and (17) imply certain functional restrictions on the variation of  $\tau$  over the surface due to our choice of complementary Stokes flow. However if  $\tau_0$  (or  $K_0, \theta_{p_0}$ ) and  $\tau_1$  (or  $K_1, \theta_{p_1}$ ) respectively denote arbitrarily selected waveforms at the front (and rear) stagnation point and at the equator then it is readily seen from equations (16) and (17) with the aid of the relations (2) that E, F, and D are given by

$$E = \frac{(1 + \tau_1 + \bar{\tau}_1 - \bar{\tau}_1 \tau_1)}{(1 + \tau_1 \bar{\tau}_1)} = (1 - K_1^2)^{\frac{1}{2}} \cos \theta_{p_1} - K_1 \tag{20}$$

$$D = \frac{(3 - \tau_0 \bar{\tau}_0 / 2)}{(1 + \tau_0 \bar{\tau}_0)} = \frac{1}{4}(7K_0 + 5) \tag{21}$$

$$F = \frac{(3 - \tau_1 \bar{\tau}_1 / 2)}{(1 + \tau_1 \bar{\tau}_1)} - D = \frac{7}{4} \{ (1 - K_1^2)^{\frac{1}{2}} \cos \theta_{p_1} - K_0 \} \tag{22}$$

A restriction on the choice of  $K_0, \theta_{p_0}$  is clearly necessary since  $q_s$  is zero at the front stagnation point. From equations (2) and (8) this requires that  $K_0 = (1 - K_0^2)^{\frac{1}{2}} \cos \theta_{p_0}$ .

Finally, the component of force on the body due to the complementary Stokes flow is simply given by integration of the stokeslets so that  $F^c = 16\pi\mu e a d$ . Thus upon integration of the stresses (11) the zero total force condition becomes:

$$\int_{\pi/2}^{-\pi/2} \frac{b \cos^2 \varphi}{[ b^2 \cos^2 \varphi + a^2 \sin^2 \varphi ]^{\frac{1}{2}}} \left\{ \frac{\partial}{\partial \varphi} (A^2 \Sigma_3) - \tan \varphi \frac{\partial}{\partial \varphi} (A^2 \Sigma_4) \right\} d\varphi \tag{23}$$

$$= - \frac{8ea}{(1-e^2)^{\frac{1}{2}} c}$$

Substituting for A,  $\Sigma_3, \Sigma_4$ , making some use of the relations (16) and (17) and integrating this becomes:

$$F = \frac{14}{k^2 \ell^2 c} \frac{ea}{(1-e^2)S_e} \quad \text{where } S_e = \frac{\sin^{-1} e - e(1-e^2)^{\frac{1}{2}}}{e^3} \quad (24)$$

We therefore have three relations (18), (19) and (24) which can be solved to find  $U$ ,  $a$  and  $\beta$  in terms of known quantities  $D$  and  $F$ . Neglecting terms which are order  $(kb)^{-1}$  since our initial restriction requires that  $kb$  be large the propulsive velocity becomes after substitution for  $E$  and  $F$  from equations (20), (21) and (22)

$$\frac{U}{c} = \frac{k^2 \ell^2}{2} [(G_e + H_e)(1 - K_1^2)^{\frac{1}{2}} \cos \theta_{p_1} - G_e K_1 - H_e K_0] \quad (25)$$

where

$$G_e = \{2e - (1-e^2) \ln \frac{1+e}{1-e}\} / 2e^3 \quad (26)$$

$$H_e = (1-e^2) \{ \sin^{-1} e - e(1-e^2)^{\frac{1}{2}} \} \{ (1+e^2) \ln \frac{1+e}{1-e} - 2e \} / 4e^6 \quad (27)$$

This propulsive velocity is readily computed for any ellipsoidal ciliate given the metachronal wave number,  $k$ , the "cilium length",  $\ell$ , the eccentricity,  $e$ , of the body shape and the ciliary beat forms at the front  $(K_0, \theta_{p_0})$  and at the mid section  $(K_1, \theta_{p_1})$ .

When  $e \rightarrow 1$  we find from equations (26) and (27) that  $G_e \rightarrow 1$  and  $H_e \rightarrow 0$  and hence we recover the infinite sheet solution of the section on the Infinite Sheet (Figure 3). On the other hand when  $e \rightarrow 0$  and the organism becomes spherical  $G_e \rightarrow 2/3$  and  $H_e \rightarrow 4/9$  and the solution of Brennen (1974) is obtained. Since the latter has a functional relationship similar to Figure 3 but with somewhat different optimum values of the propulsive velocity at slightly different  $K, \theta_p$  positions it follows that the general result (25) also has the same character as Figure 3. The first step in finding the optima of equation (25) is clearly to give  $K_0, \theta_{p_0}$  their optimum values of  $\pm 1/\sqrt{2}$  and  $0, \pi$  for antiplectic and symplectic motion respectively. Then the optimum propulsive velocities in the two directions clearly occur when  $\theta_{p_1} = \pi, 0$  and

$$K_1 = \pm G_e / [(G_e + H_e)^2 + G_e^2]^{\frac{1}{2}}$$

and the value is

$$\left| \frac{U}{c} \right|_{\text{optima}} = \frac{k^2 \ell^2}{2} [(G_e + H_e)^2 + G_e^2]^{\frac{1}{2}} + \frac{H_e}{\sqrt{2}}$$

The values of  $|U/c k^2 \ell^2|_{\text{opt}}$  and  $|K_1|_{\text{opt}}$ , as well as  $G_e$  and  $H_e$  are shown in Figure 4 as functions of the ratio of elliptical minor to major axes,  $b/a$ . We must conclude from this figure that the shape of the organism has only a minor effect on the propulsive velocity though the more rounded spherical body is somewhat better due to the additional propulsive effect mentioned previously.

The experimental data presently available in the literature is insufficiently accurate to allow evaluation of such difference. A further and most crucial difficulty in such comparisons is the fact that the present approach is based on the assumption of small wave-amplitudes (or  $k\ell < 0(1)$ ) for the envelope model; on the other hand  $k\ell$  is generally much larger as indicated in Figure 5 which represents an assimilation of data on four ciliated organisms from many sources including Sleigh(1962), Parducz (1966), Jahn and Bovee (1967), Machemer (1972), Tamm (1972), Winet (1973) and Preston (1972). The data and some non-linear considerations suggest that the factor  $k^2 \ell^2 / 2$  in the present prediction for the propulsive velocity is the linearized equivalent of  $(1 + k^2 \ell^2)^{\frac{1}{2}} - 1$ ; as can be seen from Figure 5 such a functional dependence correlates well with the observations.

#### THRUST PRODUCED BY RESTRAINED ORGANISMS

The ciliary propulsion system of a particular micro-organism is clearly called upon to perform a number of tasks and quite apart from evolutionary arguments one cannot conclude that optimum rectilinear propulsion is necessarily the most important aspect of the propulsion system. Indeed the ability to maneuver and accelerate may be of equal or greater importance. A measure of such ability is clearly the thrust which an organism can generate when its movement is restrained by some extraneous agent. This thrust is readily computed from the equations of the last section; setting  $U$  equal to zero the thrust,  $T$ , in the negative  $x$  direction is

$$T = 2\pi\mu\omega k^2 \ell^2 a [(1-e^2)S_e] [(1-K_1^2)^{\frac{1}{2}} \cos \theta_{p_1} - K_0]$$

The first conclusion we must draw from this result is that the maximum thrust occurs for ciliary beat patterns,  $K_0$ ,  $\theta_{p_0}$ ,  $K_1$ ,  $\theta_{p_1}$  which are different in general from those producing optimum

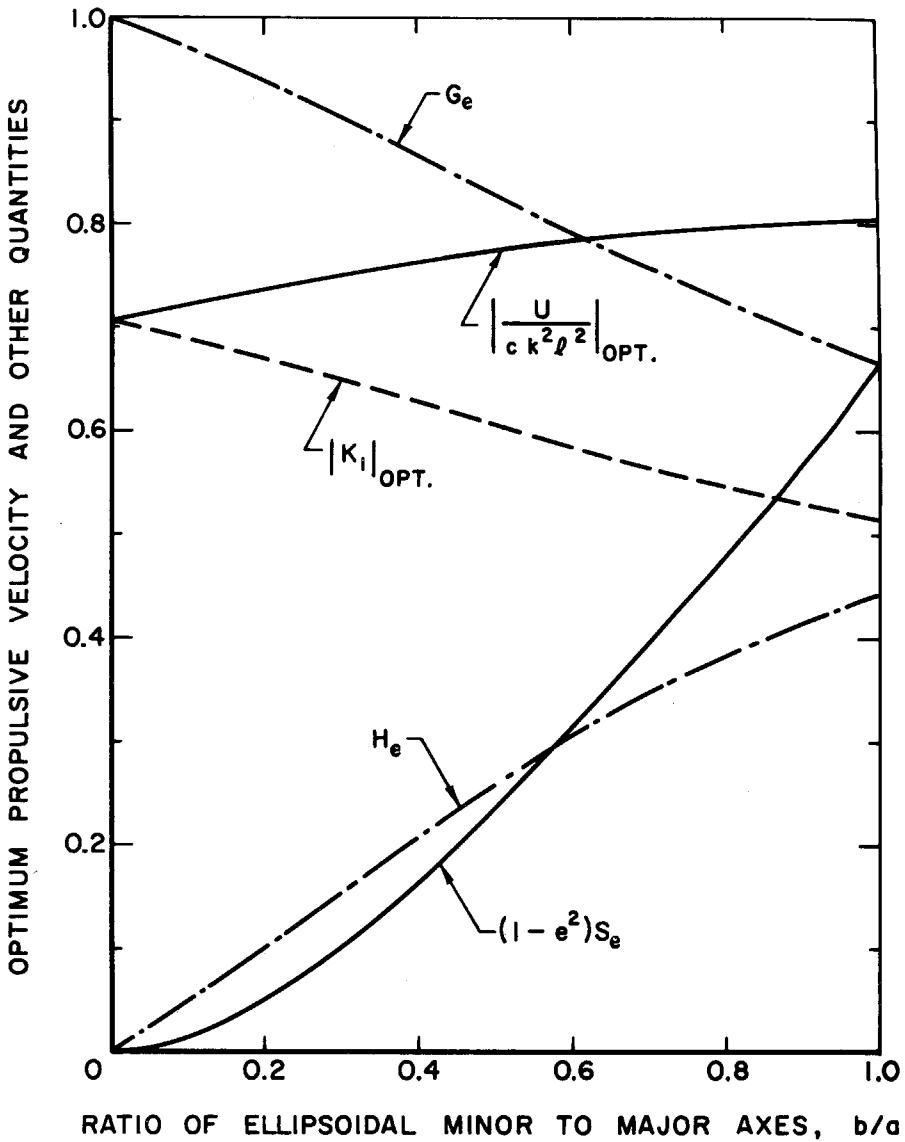


Figure 4. Variation of the optimum propulsive velocity,  $|U/ck^2 l^2|$ , for an ellipsoidal micro-organism with the axes ratio  $b/a$  and the corresponding value of  $|K_i|_{opt}$ . Also shown are the functions  $G_e$ ,  $H_e$  and  $(1-e^2)S_e$  the last being proportional to the maximum thrust which a restrained organism can generate.

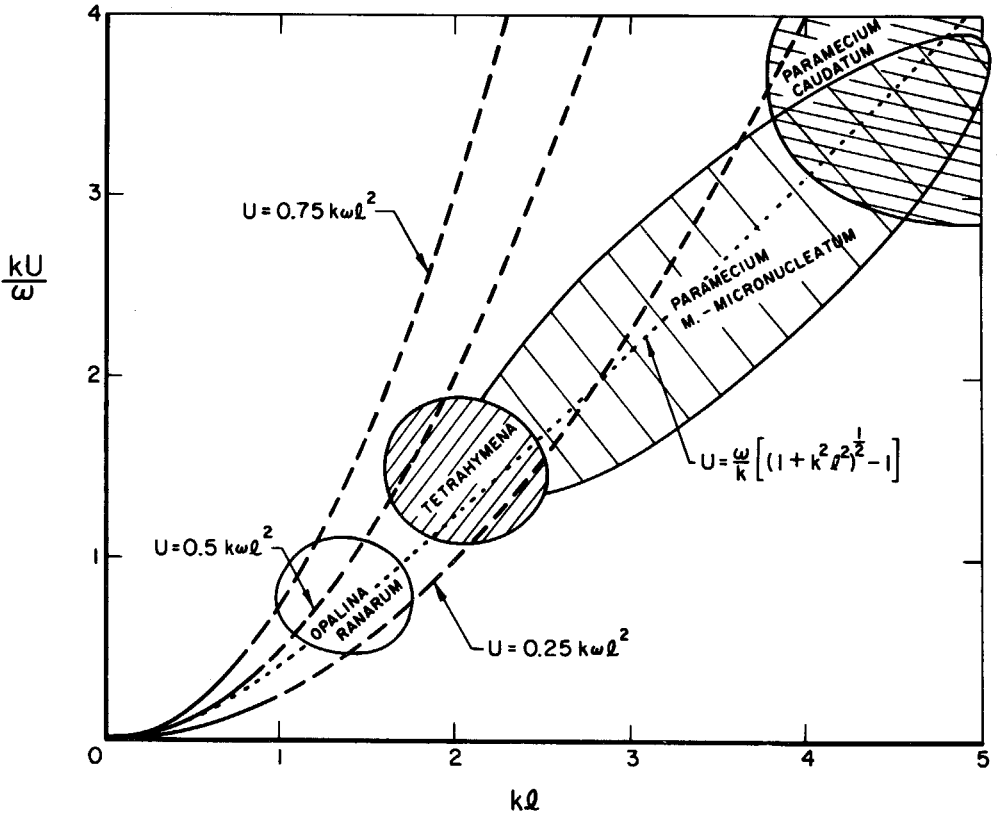


Figure 5. Non-dimensional propulsive velocities,  $U/c$ , as a function of wave amplitude,  $kl$ , with observations from a number of ciliated micro-organisms.

rectilinear propulsion. Indeed the primary variation of  $T$  with the beat pattern is given by the function  $(1 - K^2)^{1/2} \cos \theta_p$  which is plotted in Figure 6 for contrast with Figure 3. Optimum thrusts for latent symplectic ( $T = \text{positive}$ ) and latent antiplectic motion occur at  $K_1 = 0$ ,  $\theta_{p1} = 0$ ,  $K_0 = \pm 1/\sqrt{2}$  and  $\theta_{p0} = \pi, 0$  respectively and the magnitude of  $T$  is

$$|T|_{\max} = (2 + \sqrt{2})\pi\mu\omega k l^2 a(1 - e^2)S_e$$

Finally and most significantly we observe the implications of the eccentricity factor  $(1 - e^2)S_e$  which as shown in Figure 4 varies from 0 for  $b/a = 0$  to  $2/3$  at  $b/a = 1$ . Hence the surprising result that a more rounded or spherical organism is potentially

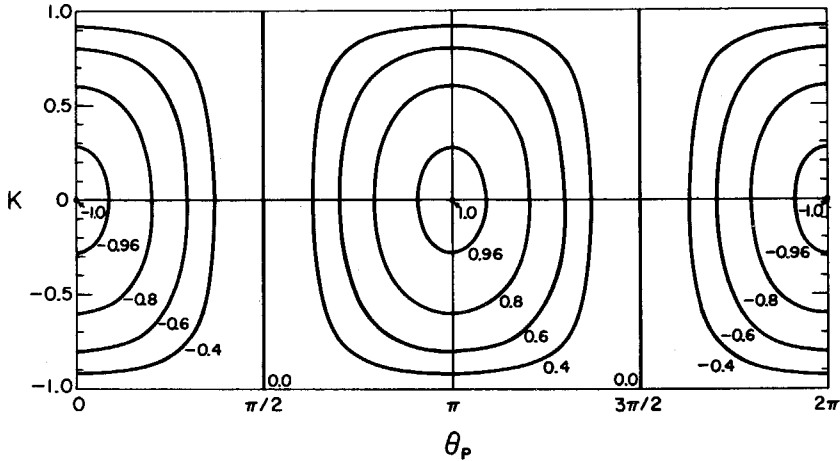


Figure 6. Variation of the function  $(1-K^2)^{\frac{1}{2}} \cos \theta_p$  which is the primary ciliary beat feature influencing the thrust an organism can generate when restrained from rectilinear propulsion.

better at accelerating and maneuvering than a more elongated or "streamlined" organism. In contrast to the shape effect on rectilinear propulsive velocity which is relatively small, this effect on the thrust is large and should be detectable in practical observations. By way of an indication of the magnitude of  $T$  we calculate using a mass plus added mass that the initial acceleration from rest of the organisms *Opalina* and *Paramecium* should be of order 1.5 and 100 body lengths/ $s^2$  respectively. Accelerations of these magnitudes are consistent with observation.

#### ACKNOWLEDGMENTS

This work was sponsored by the National Science Foundation under grant GK-31161X and by the Office of Naval Research under contract N00014-67-A-0094-0012. The author deeply appreciates the advice and encouragement of Professor T. Y. Wu and many helpful discussions with Dr. John Blake, Dr. Allen Chwang and Dr. Howard Winet.

#### REFERENCES

- Blake, J.R. 1971a A spherical envelope approach to ciliary propulsion. *J. Fluid Mech.* 46, 199-208.

- Blake, J.R. 1971b Infinite models for ciliary propulsion. *J. Fluid Mech.* 49, 209-222.
- Blake, J.R. and Chwang, A.T. 1974 Fundamental singularities of viscous flow. Part I. The image systems in the vicinity of a stationary no-slip boundary. *J. Engineering Mathematics*, 8, 23-29.
- Blake, J.R. and Sleight, M.A. 1974a Mechanics of ciliary locomotion. *Biol. Rev.* 49, 85-125.
- Blake, J.R. and Sleight, M.A. 1974b Hydro-mechanical aspects of ciliary propulsion. Proc. Symp. Swimming and Flying in Nature, Pasadena, California, July 8-12.
- Brennen, C. 1974 An oscillating-boundary-layer theory for ciliary propulsion. *J. Fluid Mech.* 65, 799.
- Cheung, A.T.W. and Winet, H. 1974 Flow velocity profile over a ciliated surface. Proc. Symp. Swimming and Flying in Nature, Pasadena, California, July 8-12.
- Chwang, A.T. and Wu, T.Y. 1974a Hydromechanics of low-Reynolds-number flow. Part I. Rotation of axisymmetric prolate bodies. *J. Fluid Mech.* 63, 607-622.
- Chwang, A.T. and Wu, T.Y. 1974b Hydromechanics of low-Reynolds number flow. Part 2. Translation of spheroids, the nature of Stokes paradox. Submitted to *J. Fluid Mech.*
- Jahn, T.L. and Bovee, E.C. 1967 Motile behavior in protozoa. In Research in Protozoology, Vol. 1, Pergamon Press, New York.
- Lighthill, M.J. 1952 On the squirming motion of nearly spherical deformable bodies through liquids at very low Reynolds numbers. *Commun. Pure Appl. Math.* 5, 109-118.
- Machemer, H. 1972 Temperature influences on ciliary beat and metachronal coordination in Paramecium. *J. Mechanochem. Cell Motility*, 1, 57-66.
- Parducz, B. 1966 Ciliary movement and coordination in ciliates. *Internat. Rev. Cytol.* 21, 91-128.
- Preston, J.T. 1972 Determination of a continuous helical ciliary beat in Tetrahymena pyriformis and the cytotoxic effect of serum complement from normal and cystic fibrotic sera on the organism. Ph.D. Thesis, U.C.L.A.



- Sleigh, M. A. 1962 The Biology of Cilia and Flagella. Pergamon Press, London.
- Tamm, S. L. 1972 Ciliary motion in Paramecium. A scanning electron microscope study. *J. Cell Biol.* 55, 250-255.
- Taylor, G. L. 1951 Analysis of the swimming of microscopic organisms. *Proc. Roy. Soc. A*, 209, 447-461.
- Tuck, E. O. 1968 A note on a swimming problem. *J. Fluid Mech.* 31, 305-308.
- Winet, H. 1973 Wall drag on free-moving ciliated microorganisms. *J. Expt. Biol.* 59, 753-766.